Simultaneous sorption and mechanical entrapment during polymer flow through porous media

Farajzadeh, R.; Bedrikovetsky, P.; Lotfollahi, M.; Lake, L. W.

DOI
10.1002/2015WR017885

Publication date
2016

Document Version
Final published version

Published in
Water Resources Research

AGU PUBLICATIONS

Water Resources Research

RESEARCH ARTICLE
10.1002/2015WR017885

Simultaneous sorption and mechanical entrapment during polymer flow through porous media

R. Farajzadeh[1,2], P. Bedrikovetsky[3], M. Lotfollahi[4], and L. W. Lake[4]

[1]Shell Global Solutions International, Rijswijk, Netherlands, [2]Department of Geoscience and Engineering, Delft University of Technology, Delft, Netherlands, [3]Australian School of Petroleum, Adelaide University, Adelaide, South Australia, Australia, [4]Petroleum and Geosystems Engineering, University of Texas at Austin, Austin, Texas, USA

Key Points:
- Adsorption and entrapment occur simultaneously during polymer flow in porous media
- Analytical solutions are provided to assess the experimental data
- Physics of the process was fully explained

Correspondence to:
R. Farajzadeh,
r.farajzadeh@tudelft.nl

Citation:
Farajzadeh, R., P. Bedrikovetsky, M. Lotfollahi, and L. W. Lake (2016), Simultaneous sorption and mechanical entrapment during polymer flow through porous media, *Water Resour. Res.*, *52*, 2279–2298, doi:10.1002/2015WR017885.

Received 22 JUL 2015
Accepted 25 FEB 2016
Accepted article online 1 MAR 2016
Published online 26 MAR 2016

Abstract Physical adsorption and mechanical entrapment are two major causes of polymer retention in porous media. Physical adsorption is considered an equilibrium process and is often modeled by assuming a Langmuir isotherm. The outcome is a steady state pressure response because the permeability reduction is also accounted for by adsorption. However, some experimental data show gradual increase of pressure with time, implying that polymer retention is a time-dependent process. We discuss simultaneous effect of sorption and mechanical entrapment on the polymer retention in porous media. An exact solution for 1-D flow problem for the case of constant filtration coefficient and Langmuir-sorption isotherm, including explicit formulae for breakthrough concentration and pressure drop across the core is derived. The general model with a varying filtration coefficient was successfully matched with experimental data confirming the occurrence of simultaneous sorption with deep-bed filtration during polymer flow in porous media. In the absence of mechanical entrapment, the physical adsorption causes delay in the polymer front and does not affect the polymer concentration behind the front. Addition of mechanical entrapment results in slow recovery of the injected concentration at the outlet (for a varying filtration coefficient) or reaching to a steady state concentration, which is only a fraction of the injected concentration (for a constant filtration coefficient). Accurate assessment and quantification of the polymer retention requires both pressure and effluent concentration data at the outlet of the porous medium.

1. Introduction

Efficient extraction of oil from subsurface formations is largely impacted by the mobility contrast between the displacing and displaced fluids [*Bedrikovetsky*, 1993; *Lake et al*., 2014]. A favorable displacement requires the mobility of the displacing agent be less than that of the displaced fluid. The ultimate sweep efficiency is also affected by the heterogeneity of the geological formations, because the permeability contrast results in preferential flow of the injected fluid through high-permeability streaks and thus a lower sweep efficiency [*Dykstra and Parsons*, 1950; *Lake et al*., 2014].

Polymer molecules are usually added to water to increase its viscosity and hence reduce the mobility ratio between the aqueous and oleic phases in the reservoir [*Hirasaki and Pope*, 1974; *Sorbie*, 1991]. Mobility ratio is defined as the mobility (the quotient of the relative permeability and viscosity of the phase) of the injected or displacing fluid divided by that of the displaced fluid [*Dake*, 1978; *Lake et al*., 2014]. Moreover, the viscosity increase can induce a viscous pressure gradient across the layers with different permeability and partially divert the flow of the injected polymer solution from the high-permeability to the low-permeability layer, which improves the conformance [*Velza et al*., 1974; *Zaitoun et al*., 1999; *Denys*, 2003].

Success of a polymer-flooding process strongly depends on the propagation of the polymeric solution deep inside the reservoir to maintain the desired mobility control throughout the targeted pore volume [*Szabo*, 1975a,1975b; *Seright et al*., 2009; *Manichand and Seright*, 2014]. Polymer retention and degradation are two main factors that affect polymer transport through porous media [*Lee and Fuller*, 1985; *Sorbie*, 1991; *Masuda et al*., 1992; *Green and Willhite*, 1998]. Polymer retention is the result of physical adsorption of the polymer molecules on the available sites on the rock surface and mechanical entrapment [*Gogarty*, 1967; *Cohen and Christ*, 1986; *Zitha et al*., 1998].

Mechanical entrapment or deep-bed filtration occurs when pore throats block the passage of the polymer molecules or the solid particles in the polymer solution (unhydrated polymer molecules or solid particles in the solution) [*Sorbie*, 1991; *Dominguez and Willhite*, 1977; *Szabo*, 1975a,1975b; *Zitha and Botermans*, 1998; *Glasbergen et al*., 2015]. The ratio between the size of the passing molecule and the pore-throat radius is therefore an important factor [*Dann et al*., 1982; *Bengtsson and Ekere*, 2001; *Al-Abduwani et al*., 2005; *Yerramilli et al*., 2013; *Lotfollahi et al*., 2016]. The viscosity of a polymer solution depends on several parameters such as concentration of the polymer, salinity, hardness, and shear rate [*Sorbie*, 1991; *Lake et al*., 2014]. For a profitable project, it is desired to reduce the amount of the polymer added to the solution to reach a certain viscosity. Polymers with a large molecular weight are suitable for this purpose; however, such polymers are more sensitive to shear degradation compared to the polymers with lower molecular weight. Ideally, the molecules are chosen such that their retention in porous media is minimal, i.e., the polymer molecules can easily flow through the narrow channels with no blocking and entrapment [*Szabo*, 1979; *Huh et al*., 1990; *Seright et al*., 2009; *Glasbergen et al*., 2015].

The rate of polymer injection into a porous medium depends on the maximum allowable pressure. Several polymer injection pilots have recently experienced unexpected pressure rise in the injector [*Clemens et al*., 2013; *Sheng et al*., 2015; *Lotfollahi et al*., 2016]. Polymer supplies for field applications are not pure and often have a wide range of molecular sizes, although the manufacturing companies often report an average molecular weight. In practice, the polymer molecules, certainly in the industrial grade, might have wider range of size distribution [*Glasbergen et al*., 2015]. In this case, it is possible that a fraction of polymer molecules, especially in the semidilute regime where molecules are entangled, is larger than the smallest pores in the porous medium. For polymer molecules larger than the rock pore size, polymer can be captured at the pore throat, and hence reduce the permeability.

Indeed, a major consequence of the polymer retention is reduction in the rock permeability leading to rise in the pressure for a certain flow rate. It is therefore necessary to accurately predict the pressure drop along the porous medium, which can be used to obtain the rate of injection for a given solution viscosity, referred to as injectivity. Traditionally, the polymer retention is modeled with the Langmuir equation [*Sorbie*, 1991]. In such models, it is assumed that the polymer adsorption reduces the effective permeability of the rock [*Hirasaki and Pope*, 1974]. The permeability reduction is measured by a permeability-reduction factor (R), which is the ratio of the effective permeability to brine and the polymer solution. The effect of the permeability reduction is assumed to be irreversible and lasts after polymer flooding and is called residual resistance factor (R_{RF}). R_{RF} is defined as the ratio of the mobility of a brine solution before and after polymer injection. The pressure increase due to the permeability-reduction factor stops when polymer adsorption reaches its maximum level. Moreover, the polymer concentration at the outlet is estimated to be that of the injected one using these models. However, in several laboratory experiments and field tests, it has been observed that the inlet pressure continues to increase even after a long time of polymer injection [*Lotfollahi et al*., 2016]. Furthermore, in those experiments, the polymer concentration at the outlet at the breakthrough time is always less than the injected polymer concentration indicating loss of the polymer inside the porous medium.

The objective of this paper is therefore to improve the current modeling approach and to describe the physics of polymer transport in porous media considering both adsorption and mechanical entrapment. The mathematical model for polymer flow in porous media accounting for retention caused by sorption and mechanical entrapment has been presented by *Huh et al*. [1990] and *Yerramilli et al*. [2013]. In the present work, an exact solution for constant filtration coefficient and Langmuir-sorption isotherm in one-dimensional flow, including explicit formulae for the breakthrough concentration and the pressure drop across the porous medium is provided. The solution for a linear adsorption isotherm is also provided in Appendix A. A more general model with a varying filtration coefficient is successfully matched to the coreflood data, suggesting the occurrence of the simultaneous sorption with deep-bed filtration during polymer flow in porous media. The proposed model and its underlying assumptions are validated using single-phase flow experiments and can be used in future works to simulate polymer flow under two-phase flow conditions.

The structure of the paper is as follows. The analytical model and the ensuing equations are presented in section 2. Typical forms of the concentration and retention profiles along with the pressure-drop history obtained from the analytical model are discussed in section 3. In section 4, the experimental data are compared with the numerical model with the varying filtration coefficient.

2. Analytical Model for Polymer Flow With Retention and Adsorption

2.1. Governing Equations

Consider incompressible, one-dimensional flow of an aqueous polymer solution through a porous medium with polymer adsorption and mechanical entrapment. The polymer concentration is so small as to not affect the volumetric balance of the aqueous solution, i.e., the polymer effect on solvent density is ignored. The relaxation time of the nonequilibrium sorption is assumed to be negligible compared to the residence time (i.e., in the limit of very large Damköhler numbers), so the equilibrium sorption with isotherm $\hat{c}(c)$ is considered. The deep-bed-filtration formula is assumed for the polymer-entrapment rate, that is, the polymer-capture rate is proportional to the dispersion-free polymer flux cu [*Maerker*, 1973; *Szabo*, 1975a,1975b; *Huh et al*., 1990; *Zhang and Seright*, 2014; *Yerramilli et al*., 2013; *McDowell-Boyer et al*., 1986; *Lotfollahi et al*., 2016]. The proportionality coefficient is the *filtration coefficient*, in accordance with the experimental data [*Sim and Chrysikopoulos*, 1995; *Bold et al*., 2003; *Al-Abduwani et al*., 2005; *Vaz et al*., 2010]. The normalized inverse permeability $k(0,0)/k(\hat{c},\sigma)$ is a monotonically increasing function of the sum of the sorbed and the entrapped concentrations $\hat{c}$ and σ; its first partial derivatives with respect to c and σ are called the resistance or the permeability-reduction (R) factor and the formation-damage coefficient (β), respectively. Only first terms in Taylor's expansion of the normalized inverse permeability with respect to the adsorbed and entrapped concentrations are considered, which leads to

$$\frac{k(0,0)}{k(\hat{c},\sigma)} = 1 + R\hat{c} + \beta\sigma. \tag{1}$$

Consequently, the system of the governing equations for 1-D flow of a polymer solution through porous media includes:

i. Equation for mass balance of dissolved c, adsorbed $\hat{c}$, and trapped polymer σ

$$\frac{\partial(\phi c + \hat{c}(c) + \sigma)}{\partial t} + u\frac{\partial c}{\partial x} = 0, \tag{2}$$

ii. Equation of the polymer-capture rate

$$\frac{\partial \sigma}{\partial t} = \lambda(\sigma) c u, \tag{3}$$

iii. Darcy's law accounting for the permeability reduction because of the polymer sorption and entrapment expressed by equation (1)

$$u = -\frac{k_0}{\mu(c)(1 + R\hat{c} + \beta\sigma)}\frac{\partial p}{\partial x}. \tag{4}$$

Here ϕ is porosity, c, σ, and $\hat{c}$ are concentrations of flowing, entrapped, and adsorbed polymer (all expressed in mass fraction), u is flow velocity, λ (1/m) is the filtration coefficient, k_0 (m^2) is the initial permeability of the rock, and R is the resistance (or permeability reduction) factor due to polymer adsorption. It is assumed that the viscosity of the polymer solution linearly increases with the increasing polymer concentration, i.e.,

$$\mu = \mu_w(1 + mc). \tag{5}$$

The filtration coefficient can be a function of the retention concentration, reflecting the variation of the retention rate with the change of the pore space geometry. For the case of the varying filtration coefficient, the filtration coefficient is assumed to linearly depend on the retained polymer concentration, i.e., so-called blocking function [*Vaz et al*., 2010]:

$$\lambda(\sigma) = \lambda_0\left(1 - \frac{\sigma}{\sigma_{\max}}\right), \tag{6}$$

where λ_0 is the filtration coefficient at zero polymer retention, and $\sigma_{\max}$ is the maximum polymer retention. The implication of the blocking function is that the polymer retention rate decreases as the retained concentration of the polymer, σ, increases.

The case of the constant-filtration coefficient corresponds to a negligible retention concentration compared to the density of the vacant sites for capture of the polymer macromolecules—in this case, different molecules filtrate independent of each other with a constant capture probability (see *Bedrikovetsky* [2008] for a detailed discussion of this assumption).

The following dimensionless coordinates, concentrations, and coefficients are introduced

$$x_D=\frac{x}{L},\ t_D=\frac{ut}{\phi L},\ C=\frac{c}{c_0},\ S=\frac{\sigma}{\phi c_0},\ \hat{C}=\frac{\hat{c}}{\phi c_0},\ P=\frac{kp}{u\mu_w L},\ \Lambda=\lambda_0 L,\ M=c_0 m. \tag{7}$$

Subsequently, system of equations (2–4) in the dimensionless form becomes

$$\frac{\partial\left(C+\hat{C}(C)+S\right)}{\partial t_D}+\frac{\partial C}{\partial x_D}=0, \tag{8}$$

$$\frac{\partial S}{\partial t_D}=\Lambda C, \tag{9}$$

$$1=-\frac{1}{(1+MC)\left(1+R\phi c_0\hat{C}+\beta\phi c_0 S\right)}\frac{\partial P}{\partial x_D}, \tag{10}$$

The Langmuir adsorption isotherm [see *Sorbie*, 1991; *Lake et al*., 2003] is considered

$$\hat{C}=\frac{bC}{1+bC}\hat{C}_{\max}, \tag{11}$$

where $\hat{C}_{\max}$ is the maximum dimensionless adsorbed-polymer concentration (as defined on a pore volume basis, see equation (7)) and parameter b represent the nonlinearity of the isotherm [*Lake et al*., 2003]. Function $\hat{C}$ is monotonically increasing and convex. Examples are shown on Figure 1.

A solution to the system of three equations (8–10) determines three unknowns: polymer concentration in the aqueous solution C, concentration of mechanically entrapped polymer S, and pressure P. Nevertheless, equations (8) and (9) can be solved separately from equation (10). The solutions can then be used to calculate the pressure using equation (10).

The initial condition for the system of equations (8) and (9) corresponds to the absence of polymer before injection:

$$t_D=0 : C=S=0. \tag{12}$$

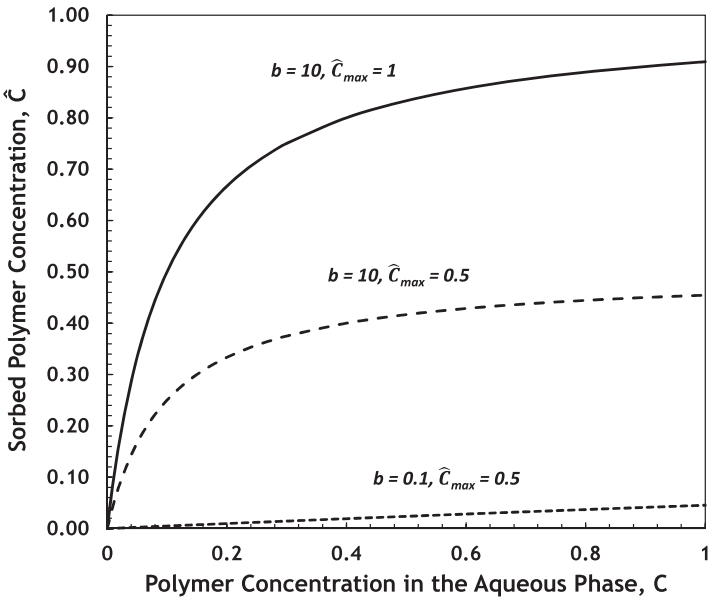

Figure 1. Langmuir isotherm for adsorption of polymer using equation (11), adapted from *Lake et al*. [2003].

Inlet boundary condition corresponds to the injection of the aqueous-polymer solution with a constant concentration, i.e.,

$$x_D=0 : C=1. \tag{13}$$

This is a typical Goursat problem [*Soltanov*, 2013] in which the inlet $x_D=0$ is a characteristic line. Therefore, because the equations are decoupled and equation (9) is local in space, a boundary condition is not needed for S.

In the following section, the exact solution for the case with a constant filtration coefficient is provided. The case of varying $\lambda(\sigma)$ is solved numerically. Therefore, equation (6) is

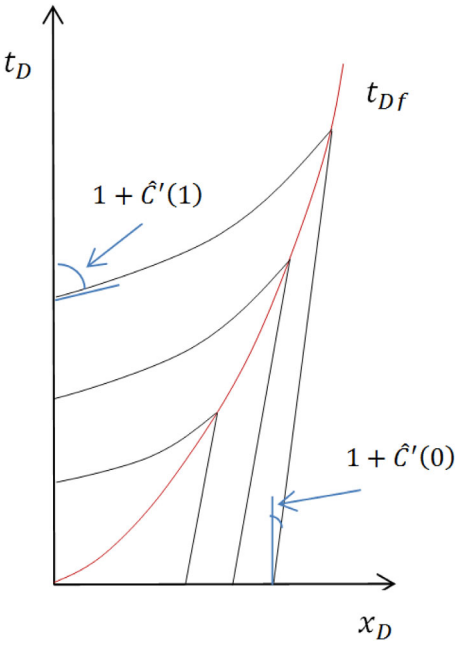

Figure 2. Characteristic trajectories of $t_D = t_f(x_D)$.

combined with equation (2) including the dispersion term. In the presence of polymer, the viscosity of the aqueous phase is calculated from Carreau's model [*Carreau*, 1968]. These equations along with the pressure equation (4) are discretized using the finite difference approach and solved in IMPEC (implicit pressure and explicit concentration) scheme. The details of the equations and the numerical scheme are discussed in Appendix B. To minimize the effect of dispersion, the grid size is chosen such that the solution of the polymer concentration becomes independent of the number of grid blocks.

2.2. Exact Solution for One-Dimensional Polymer Flow With a Constration Filtration Coefficient

Consider the system of equations (8) and (9) subject to the initial and boundary conditions described by equations (12) and (13). Substituting equation (9) into equation (8) and further differentiation of equation (8) yields

$$\frac{\partial\left(C+\hat{C}(C)\right)}{\partial t_D}+\frac{\partial C}{\partial x_D}=-\Lambda C, \tag{14a}$$

$$\left(1+\hat{C}'^{(C)}\right)\frac{\partial C}{\partial t_D}+\frac{\partial C}{\partial x_D}=-\Lambda C. \tag{14b}$$

Equation (14a) describes the polymer transport in porous media in the domain of concentration $C(x_D,t_D)$ continuity. The mass balance (Hugoniot-Rankine) condition is assumed at the shock:

$$\frac{dx_{Df}}{dt_D}=\frac{[C]}{[C]+[\hat{C}]}, \tag{14b-1}$$

where the jump of a physical value A is the difference between its values upstream and downstream of the shock front, $[A]=A^{+}\text{-}A^{-}$.

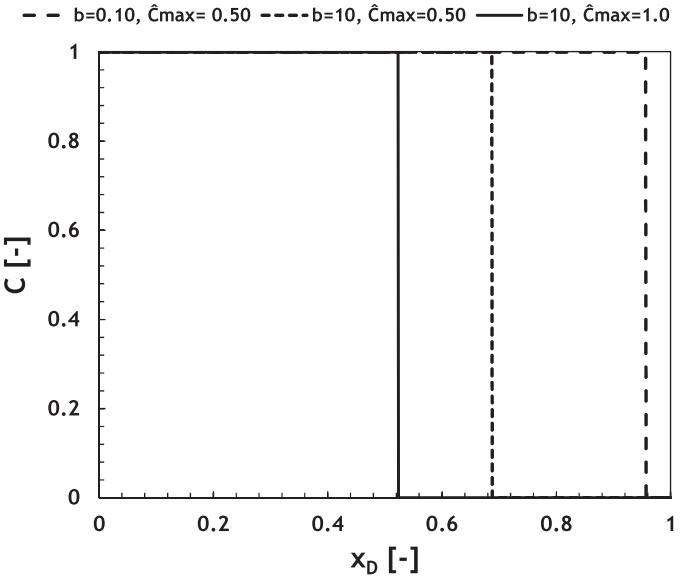

Figure 3. Effect of adsorption only on the concentration profile. The concentration profiles are plotted after 1.0 pore volume (PV) of polymer injection using the corresponding adsorption isotherms in Figure 1. Adsorption only delays the front propagation and has no effect on the polymer concentration behind the front.

The weak solution must be stable with respect to the small perturbations, yielding the following Lax's conditions [*Landau and Lifschitz*, 1987; *Barenblatt et al*, 1989]:

$$\frac{1}{1+\hat{C}'(C^{+})}<\frac{dx_{Df}}{dt_D}<\frac{1}{1+\hat{C}'(C^{-})}. \tag{14b-2}$$

The Oleinik's condition for stability with respect to finite-size perturbations is [*Barenblatt et al*., 1989; *Bedrikovetsky*, 1993]

$$\frac{dx_{Df}}{dt_D}<\frac{C-C^{-}}{(C-C^{-})+\left(\hat{C}(C)-\hat{C}(C^{-})\right)}, \tag{14b-3}$$

where C is an arbitrary value from the interval between the values C^{+} and C^{-}. A convex form for the adsorption curve is assumed here

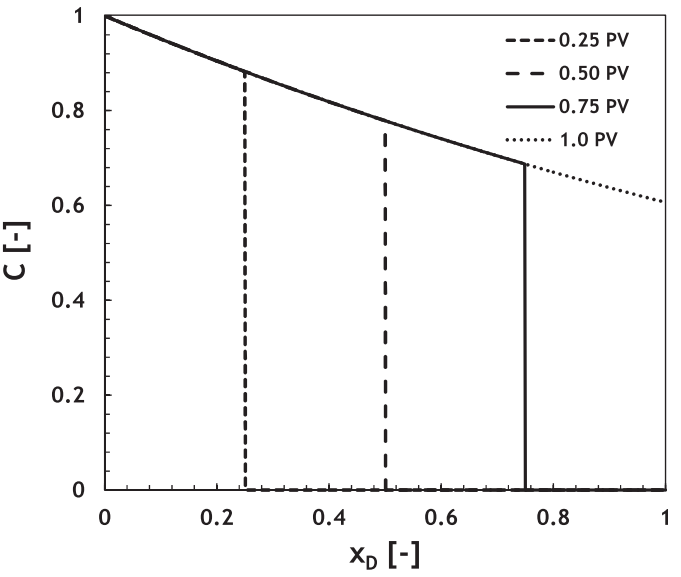

Figure 4. Flowing polymer concentration for the case with a constant filtration coefficient as a function of time (or pore volume injected). No adsorption is considered ($L = 1$ m, $\Lambda = 0.5$, and $\hat{C}_{max} = 0$).

and therefore the criterion given by equation (14b-3) is fulfilled.

The weak solution fulfilling the shock conditions (14b-1)–(14b-3) is unique and stable with respect to the small perturbations of the concentration $C(x_D, t_D)$. The exact solution presented next fulfills the conditions (14b-1)–(14b-3).

The solution of the homogeneous equation (14b) (with zero right side) subject to the initial and boundary conditions expressed in equations (12) and (13) is given by a shock wave

$$C(x_D,t_D)=\begin{cases} 1, & 0<\dfrac{x_D}{t_D}<\dfrac{1}{1+\hat{C}(1)} \\ 0, & \dfrac{1}{1+\hat{C}(1)}<\dfrac{x_D}{t_D}<\infty \end{cases} \tag{14c}$$

The shock described by equation (14c) propagates along the trajectory $t_D = t_f(x_D)$, shown in Figure 2.

The characteristic form of the first-order partial differential equation (14b) is

$$\frac{dt_D}{dx_D}=1+\hat{C}'(C), \tag{15}$$

$$\frac{dC}{dx_D}=-\Lambda C, \tag{16}$$

where $t_D = t_D(x_D)$ is the characteristic equation.

Equation (16) with the boundary condition equation (13) behind the front (for $t_D > t_{Df}(x_D)$) is solved by separation of the variables to obtain the polymer concentration in the aqueous solution:

$$C=e^{-\Lambda x_D}. \tag{17a}$$

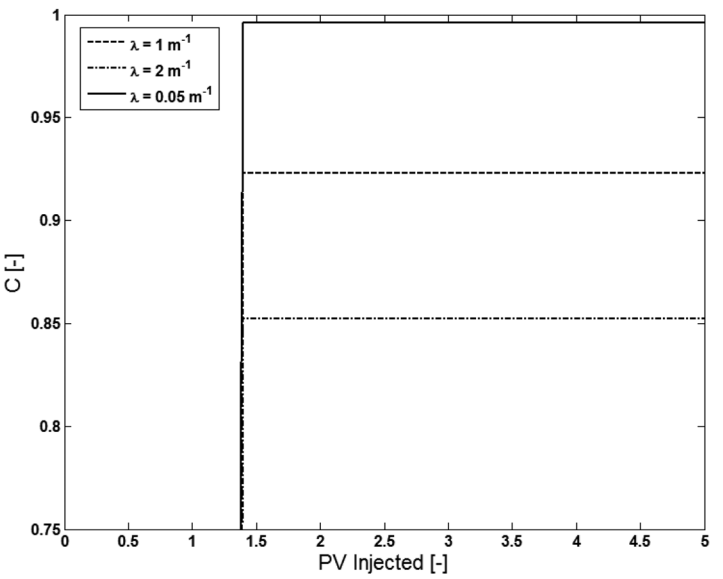

Figure 5. Effect of filtration rate on the effluent concentration history. Higher the filtration rate, lower the recovered concentration at the outlet. The parameters are listed in Table 1.

Derivation of the characteristic form of the first-order partial differential equation (14b) along the characteristics $x_D = x_D(t_D)$ ahead of the front $t_D < t_{Df}(x_D)$, and solving it yields to zero concentration. Therefore, the polymer concentration is:

$$C(x_D,t_D)=\begin{cases} e^{-\Lambda x_D}, & t_D \geq t_{Df}(x_D) \\ 0, & t_D < t_{Df}(x_D) \end{cases} \tag{17b}$$

The derivative of the Langmuir-sorption isotherm (equation (8)) is

Table 1. Parameters Used to Calculate Curves in Figure 5

Parameter	Value	Unit	Parameter	Value	Unit
L	0.08	m	μ_w	0.6	cP
K	2.40×10^{-12}	m^2	c_0	2000	ppm
ϕ	0.28		R	1.5×10^3	
U	3.30×10^{-6}	m/s	$\hat{C}_{max}$	2.2×10^{-5}	
μ_p	100	cP	b	1500	

$$\hat{C}' = \frac{b\hat{C}_{max}}{(1+bC)^2}. \tag{18}$$

Substituting solution in equation (17b) into equation (15) yields

$$\frac{dt_D}{dx_D} = 1 + \frac{b\hat{C}_{max}}{(1+bC)^2}. \tag{19a}$$

Integration of equation (19a) in x_D from zero yields the trajectory of the characteristic line $t_D = t_D(x_D)$ crossing the ordinate axis at time t_0:

$$t_D = t_0 + x_D - \frac{b\hat{C}_{max}}{\Lambda}\left(-\ln\left(1+be^{-\Lambda x_D}\right) + \ln(1+b) + \frac{1}{1+be^{-\Lambda x_D}} - \frac{1}{1+b} - \Lambda x_D\right). \tag{19b}$$

The phase portrait for the characteristic lines is shown in Figure 2.

Consider first the characteristic lines that start at $x_D = 0$. According to equation (17), concentration C decreases monotonically along the characteristic line from $C = 1$ at $x_D = 0$ to $C = 0$ with x_D tending to infinity. Therefore, the slope of the characteristic curve increases from $1 + b\hat{C}_{max}/(1+b)^2$ at $x_D = 0$ to $1 + b\hat{C}_{max}$ with x_D tending to infinity.

The characteristic lines starting at the ordinate axis $t_D = 0$ have the slope that exceeds the slope of those starting at $x_D = 0$. Consequently, both families of the characteristic curves intersect, i.e.,

$$\frac{dt_D}{dx_D} = 1 + \hat{C}'(C) = 1 + \frac{b\hat{C}_{max}}{\left(1+be^{-\Lambda x_D}\right)^2} < 1 + \hat{C}'(0) = 1 + b, \tag{20}$$

This yields that the solution must contain a shock front. Its trajectory $t_f(x_D)$ separates the zone with $C = 0$ ahead of the front and the zone behind, where the concentration field is determined by equation (17). Therefore, the concentration ahead of the front is equal to zero. The expression for the front speed follows from the Hugoniot-Rankine condition of the mass balance on the front

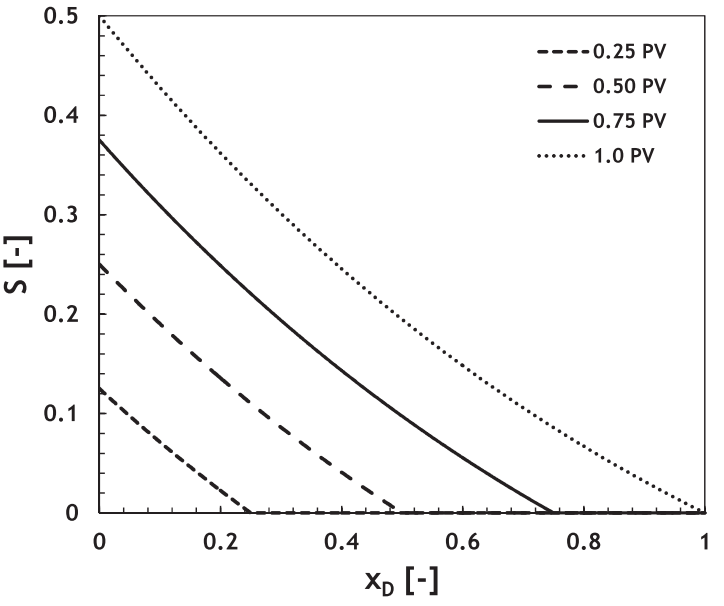

Figure 6. Retained polymer concentration for the case with a constant filtration coefficient ($L = 1$ m, $\Lambda = 0.5$, and $\hat{C}_{max} = 0$).

$$\frac{dt_{Df}}{dx_D} = 1 + \frac{\hat{C}(C^-)}{C^-}. \tag{21}$$

Substitution of equation (17a) into equation (21) yields

$$\frac{dt_{Df}}{dx_D} = 1 + \frac{b\hat{C}_{max}}{1+be^{-\Lambda x_D}}, \tag{22}$$

and further integration in x_D leads to an expression for the front trajectory

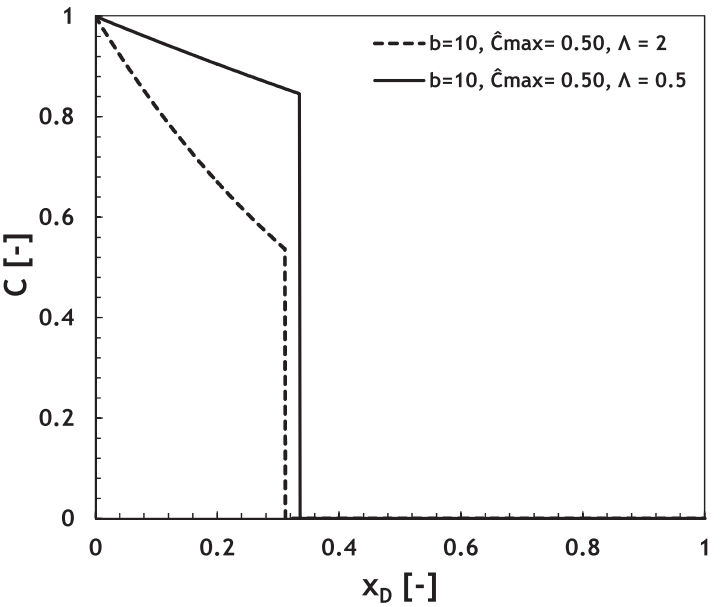

Figure 7. Effect of mechanical entrapment on the propagation of polymer front. The front is further delayed because of entrapment of the polymer. The concentration profile is plotted after 0.50 pore volume (PV) of polymer injection.

$$t_{Df}=x_D+b\hat{C}_{\max}\int_0^{x_D}\frac{dx}{1+be^{-\Lambda x_D}}=x_D\left(1+b\hat{C}_{\max}\right)+\frac{b\hat{C}_{\max}}{\Lambda}\ln\left(\frac{1+be^{-\Lambda x_D}}{1+b}\right). \tag{23}$$

The polymer breakthrough at the core outlet occurs at:

$$t_{BT}=1+b\hat{C}_{\max}+\frac{b\hat{C}_{\max}}{\Lambda}\ln\left(\frac{1+be^{-\Lambda}}{1+b}\right) \tag{24}$$

A notable feature of the problem with a constant filtration coefficient in equation (3) is the steady state concentration profile behind the front, equation (17). Therefore, the front trajectory is independent of the equation of the characteristic line in equation (19b). Time variation of the injected concentration in the inlet boundary condition, described by equation (13), results in the solution of the system of the transcendent equations (17), (19b), and (20) whose solution gives the front trajectory. For example, the system (17, 19b, and 20) can be solved for the case of the polymer-slug injection followed by the water drive in order to find the trajectory of the rear slug front.

The concentration profile is given by equations (17b) and (22):

$$C(x_D,t_D)=\begin{cases} e^{-\Lambda x_D}, & t_D>x_D\left(1+b\hat{C}_{\max}\right)+\dfrac{b\hat{C}_{\max}}{\Lambda}\ln\left(\dfrac{1+be^{-\Lambda x_D}}{1+b}\right) \\ 0, & t_D<x_D\left(1+b\hat{C}_{\max}\right)+\dfrac{b\hat{C}_{\max}}{\Lambda}\ln\left(\dfrac{1+be^{-\Lambda x_D}}{1+b}\right) \end{cases}. \tag{25}$$

Integrating both sides of equation (9) in t_D from zero results in an expression for the concentration of the entrapped polymer behind the front ($t_D > t_{Df}$). Because concentration C is zero ahead of the front, the integration starts at $t_D=t_{Df}$:

$$S(x_D,t_D)=\Lambda(t_D-t_{Df}(x_D))e^{-\Lambda x_D} \tag{26}$$

Substitution of equation (23) into equation (26) leads to

$$S(x_D,t_D)=\Lambda\left(t_D-x_D\left(1+b\hat{C}_{\max}\right)-\frac{b\hat{C}_{\max}}{\Lambda}\ln\left(\frac{1+be^{-\Lambda x_D}}{1+b}\right)\right)e^{-\Lambda x_D} \tag{27}$$

2.3. Calculation of the Pressure Drop

Explicit formulae for the flowing and entrapped polymer concentrations C and S allow calculating pressure drop across the porous medium during polymer injection. Expression of the pressure drop from equation (10) and integration in x_D yields

$$\Delta P=\int_0^1(1+MC)\left(1+R\phi c_0\hat{C}+\beta\phi c_0 S\right)dx_D. \tag{28}$$

Because no polymer is present ahead of the front, $C = 0$, $\hat{C} = 0$, and $S=0$, therefore, the pressure drop before the breakthrough is

$$\Delta P=\int_0^{x_{Df}}(1+MC)dx_D+R\phi c_0\int_0^{x_{Df}}(1+MC)\hat{C}dx_D+\beta\phi c_0\int_0^{x_{Df}}(1+MC)Sdx_D. \tag{29}$$

The first integral on the right hand side of equation (29) is equal to

$$\int_0^{x_{Df}}(1+MC)dx_D=x_{Df}+\frac{M}{\Lambda}\left(1-e^{-\Lambda x_{Df}}\right). \tag{30}$$

The second integral leads to

$$\int_0^{x_{Df}}(1+MC)\hat{C}dx_D=\frac{M\hat{C}_{\max}}{\Lambda}\left(1-e^{-\Lambda x_{Df}}\right)+\frac{\hat{C}_{\max}}{\Lambda}\left(\frac{M}{b}-1\right)\ln\left(\frac{1+be^{-\Lambda x_{Df}}}{1+b}\right). \tag{31}$$

The third integral in the right hand side of equation (28) before the polymer breakthrough is

$$\int_0^{x_{Df}}(1+MC)Sdx_D=\frac{\hat{C}_{\max}}{\Lambda}\left(1+be^{-\Lambda x_{Df}}+\frac{M}{2}\left(be^{-2\Lambda x_{Df}}-\frac{1}{b}\right)\right)\ln\left(\frac{1+be^{-\Lambda x_{Df}}}{1+b}\right)$$
$$+x_{Df}\left(1+b\hat{C}_{\max}\right)\left(1+\frac{M}{2}e^{-\Lambda x_{Df}}\right)e^{-\Lambda x_{Df}}+\left(1-e^{-\Lambda x_{Df}}\right)\left(t_D-\frac{1}{\Lambda}\left(1+\frac{M\hat{C}_{\max}}{2}\right)\right)+\frac{M}{2}\left(1-e^{-2\Lambda x_{Df}}\right)\left(t_D-\frac{1}{2\Lambda}\right). \tag{32}$$

Therefore, the pressure drop before the breakthrough can be calculated from

$$\Delta P=x_{Df}+\frac{M}{\Lambda}\left(1-e^{-\Lambda x_{Df}}\right)+R\phi c_0\left[\frac{M\hat{C}_{\max}}{\Lambda}\left(1-e^{-\Lambda x_{Df}}\right)+\frac{\hat{C}_{\max}}{\Lambda}\left(\frac{M}{b}-1\right)\ln\left(\frac{1+be^{-\Lambda x_{Df}}}{1+b}\right)\right]$$
$$+\beta\phi c_0\left[\frac{\hat{C}_{\max}}{\Lambda}\left(1+be^{-\Lambda x_{Df}}+\frac{M}{2}\left(be^{-2\Lambda x_{Df}}-\frac{1}{b}\right)\right)\ln\left(\frac{1+be^{-\Lambda x_{Df}}}{1+b}\right)\right.$$
$$\left.+x_{Df}\left(1+b\hat{C}_{\max}\right)\left(1+\frac{M}{2}e^{-\Lambda x_{Df}}\right)e^{-\Lambda x_{Df}}+\left(1-e^{-\Lambda x_{Df}}\right)\left(t_D-\frac{1}{\Lambda}\left(1+\frac{M\hat{C}_{\max}}{2}\right)\right)+\frac{M}{2}\left(1-e^{-2\Lambda x_{Df}}\right)\left(t_D-\frac{1}{2\Lambda}\right)\right]. \tag{33}$$

After the polymer breakthrough, the integration in x_D is performed from zero to one, and the pressure is calculated by inserting $x_{Df}=1$ in equation (33), i.e.,

$$\Delta P=1+\left(\frac{M}{\Lambda}+\beta\phi c_0t_D-\frac{\beta\phi c_0}{\Lambda}\left(1+\frac{M\hat{C}_{\max}}{2}\right)+R\phi c_0\frac{M\hat{C}_{\max}}{\Lambda}\right)\left(1-e^{-\Lambda}\right)$$
$$+\left[R\phi c_0\frac{\hat{C}_{\max}}{\Lambda}\left(\frac{M}{b}-1\right)+\beta\phi c_0\frac{\hat{C}_{\max}}{\Lambda}\left(1+be^{-\Lambda}+\frac{M}{2}\left(be^{-2\Lambda}-\frac{1}{b}\right)\right)\right]\ln\left(\frac{1+be^{-\Lambda}}{1+b}\right)\right] \tag{34}$$
$$+\beta\phi c_0\left[\left(1+b\hat{C}_{\max}\right)\left(1+\frac{M}{2}e^{-\Lambda}\right)e^{-\Lambda}+\frac{M}{2}\left(1-e^{-2\Lambda}\right)\left(t_D-\frac{1}{2\Lambda}\right)\right].$$

Equations (33) and (34) correspond to the pressure drop before and after polymer breakthrough, respectively.

3. Qualitative Behavior of the Polymer Flow With a Constant Filtration Coefficient

Figure 3 shows the polymer concentration in the aqueous phase for the case of adsorption only. The details of this case have been discussed in *Lake et al.* [2003]; nevertheless, for the sake of coherence, the main features of this solution are briefly reviewed. The profile is plotted after 1 pore volume (PV) of polymer injection. The solution consists of a shock from the injection concentration to the initial concentration. The most important feature of the adsorption process is delaying of the front propagation, i.e., sorption does not affect the polymer concentration behind the front. This indicates that, in the absence of dispersion, at the outlet of the porous medium, the polymer concentration will see a jump from zero to unity when adsorption is the only cause of the polymer retention in porous media. The increase in b and $b\hat{C}_{\max}$ (keeping the other parameters constant) results in further retardation of the shock front. The inclusion of dispersion in

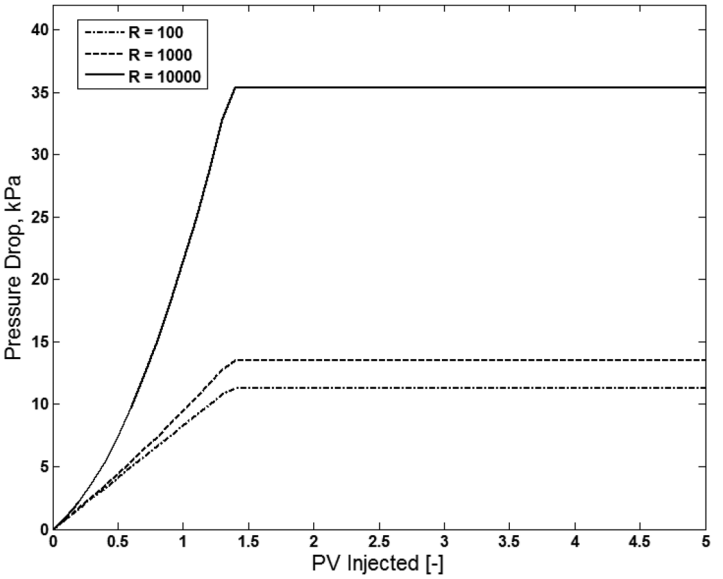

Figure 8. Effect of *R*, i.e., the permeability-reduction factor due to adsorption (equation (4)) on the pressure history of a core initially saturated with water and then displaced by a polymer soultion. The parameters in Table 1 were used to obtain the curves.

the equations spreads the concentration front and has no influence on the concentration upstream and downstream of the front.

Figure 4 shows the profile of the polymer concentration in the aqueous phase at different times for the case with filtration only. This is obtained by putting adsorption parameters to zero in equation (25). The solution consists of a continuous solution followed by a shock to the initial condition ($C=0$ in this case). The polymer concentration decreases along the distance from inlet of the porous medium until the position of the shock. The reduction of the polymer concentration reduces the viscosity of the aqueous solution and has a detrimental effect on its displacement efficiency. The viscosity at the front will be the smallest, which is of course undesired because losing mobility at the front can lead to an unstable displacement. It is noticeable that in this case, the viscosity of the flowing solution (*displacing* agent) will be always less than the injected viscosity.

An important feature of this solution is the steady state concentration of the flowing polymer, i.e., the flowing polymer concentration behind the front does not change with time. The consequence of this behavior is a constant polymer concentration at the outlet of the porous medium after polymer breakthrough. Indeed, for a constant filtration coefficient, the polymer concentration at the outlet will not reach the injected concentration and depending on the value of the filtration coefficient, only a fraction of polymer will be recovered at the outlet. This means that the entire polymer newly arriving at any arbitrary point x_D is captured in the pore throat. This is shown in Figure 5 for different values of the filtration coefficient. The other parameters are listed in Table 1. The amount of the recovered polymer at the outlet increases with decreasing λ, as more polymer is retained inside the porous medium when the value of λ (or entrapment rate) increases. Moreover, as it follows from equation (9), in this case the retained concentration accumulates proportionally to time.

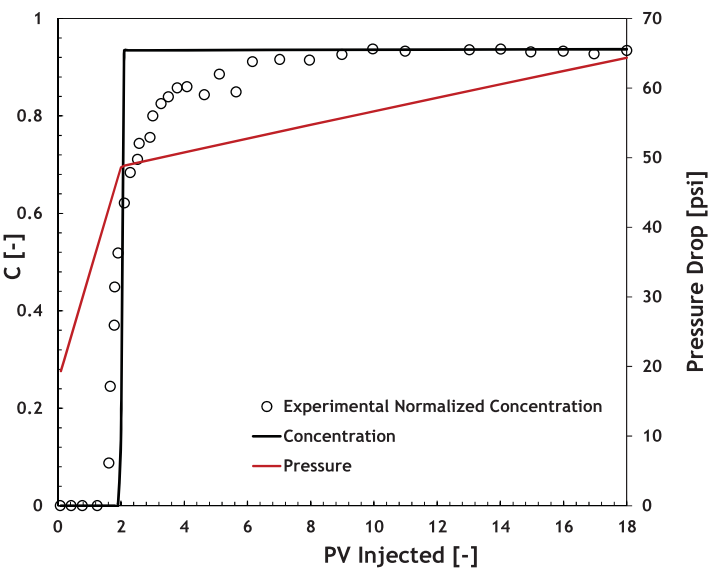

Figure 9. Comparison of the experimetal data (concentration) with the model with a constant filtration coefficient. The concentration in the outlet does not reach the feed concentration, instead it plateaus at a certain fraction of the inlet concentration after polymer breakthrough. The parameters in Table 1 along with $\lambda=0.053\ m^{-1}$ were used to obtain the curves.

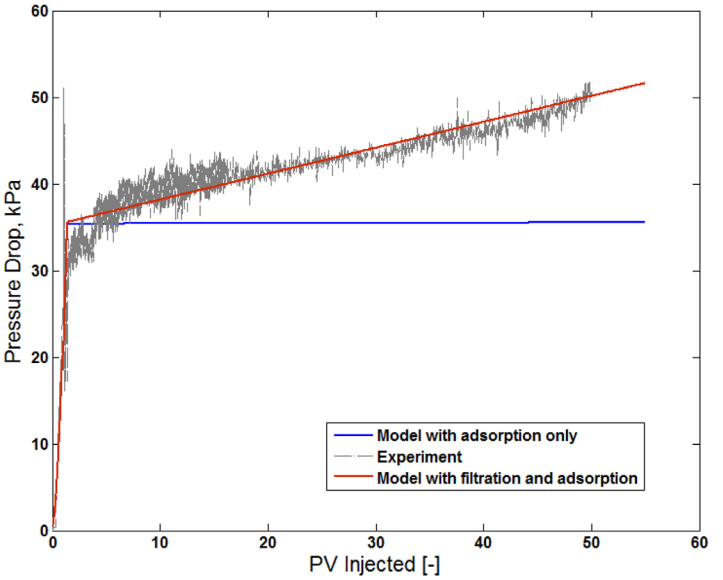

Figure 10. Comparison of the pressure-history data with the model. The adsorption only model does not predict the pressure rise after breakthrough ($\lambda = 0.053$ m^{-1}, $\beta = 4000$, and $R = 200$).

Figure 6 shows the profile of the entrapped polymer concentration. The entrapment of the polymer is largest at the inlet of the porous medium and decreases along the porous medium, in accordance with equation (27). Moreover, the entrapped concentration of the polymer increases as more polymer solution is injected.

When mechanical entrapment is the only cause of polymer retention in porous media, polymer breakthrough occurs at 1 PV indicating that, in the absence of adsorption, entrapment of polymer does not influence polymer-propagation rate. This is the consequence of inserting $\hat{C}_{max} = 0$ in equation (24). However, when simultaneous effects of adsorption and filtration are accounted for, polymer breakthrough is further delayed by the entrapment mechanism. Figure 7 demonstrates an example of the flowing-concentration profile for the case with the combined effect of adsorption and entrapment. For identical adsorption parameters, the fronts travel with different speeds for two different filtration coefficients. The front moves slower when a larger λ is considered. Therefore, entrapment contributes to the frontal loss of the polymer as well as to the viscosity loss behind the front, while adsorption is only responsible for the frontal loss of the polymer.

Apart from concentration, polymer retention affects the pressure behavior in porous media. It is known that injection of a polymer-free aqueous solution before and after polymer results in different pressure drops along the porous medium. In fact, the pressure drop becomes larger after injection of the polymer solution. The effect of R (or permeability-reduction factor) on the pressure history is shown in Figure 8. The curves are calculated using the parameters in Table 1. The increase in the value of R has two main effects on the pressure history: it increases the slope of the pressure curve and shifts the plateau pressure to higher values. It is noticeable that once the polymer breakthrough occurs, the pressure remains stable. The value of R has no effect on the breakthrough time or the concentration profile.

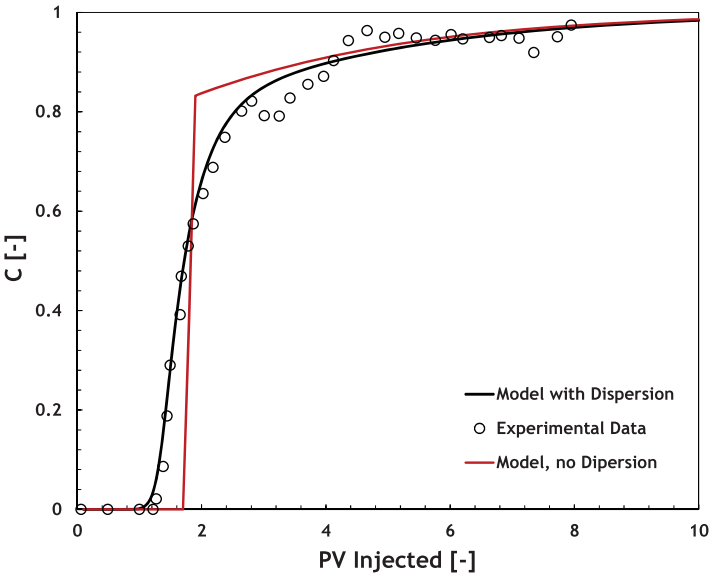

Figure 11. Comparison of the model with the experimental data (Xanthan flow through rock with permeability of 37 mD at intersitial velocity of 5 ft/d). The fit is obtained by setting $\lambda_0 = 0.5$ ft^{-1} and $\sigma_{max} = 0.018$ m^3/m^3. Data from *Huh et al.* [1990].

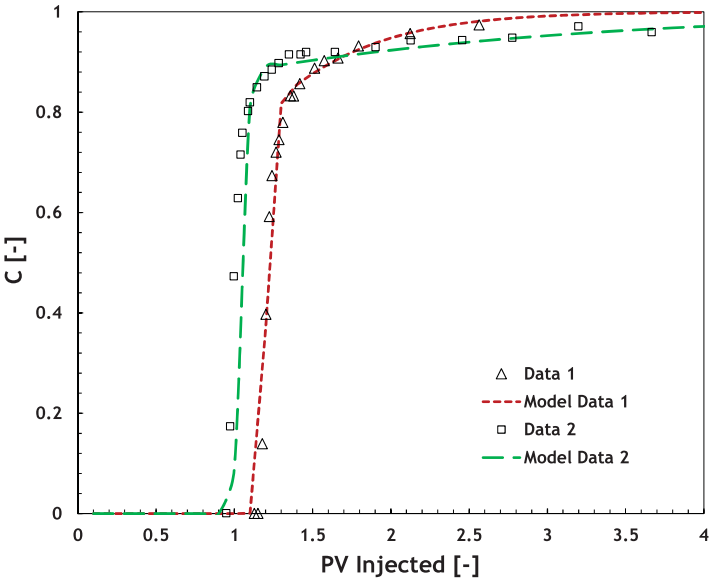

Figure 12. Comparison of the model with the experimental data (hydrolyzed polyacrylamide, HPAM, flow through a core). Data 1: $k = 234$ mD, $v = 1$ m/d, and $c_0 = 489$ ppm. The fit to Data 1 is obtained by setting $\lambda_0 = 0.40$ ft^{-1} and $\sigma_{max} = 1.0 \times 10^{-5}$ m^3/m^3. Data 2: $k = 166$ mD, $v = 1$ m/d, and $c_0 = 187$ppm. The fit is obtained by setting $\lambda_0 = 0.25$ ft^{-1} and $\sigma_{max} = 6.0\ 10^{-5}$ m^3/m^3. Data from *Dominguez and Willhite* [1977].

When mechanical entrapment is also considered, the pressure continuously increases. The rate of the pressure rise depends on the value of β in equation (4). This is shown with a red curve on Figure 9. The mismatch between the data and the model around the breakthrough time is most likely due to the core heterogeneity and dispersion that are not accounted for in the analytical model. Moreover, in Figure 10, the results of the model are compared to the experimental data. The blue line only assumes adsorption, which does not predict the gradual pressure rise after the polymer breakthrough. The data adequately fit the model when the combined effects of entrapment and adsorption are considered. Accurate estimation of the polymer retention requires both concentration and pressure histories. For example, in Figure 9, one is able to obtain the match between the concentration data and the model by tuning the value of $\hat{C}(\hat{C}_{max}, b)$, R, and Λ (see Table 1 for other parameters). However, to get the value of β, pressure data are also required. For a constant filtration coefficient, the pressure keeps increasing until an external filter cake is formed at (or near) the sand face, after which the slope increases [*Lotfollahi et al*., 2016].

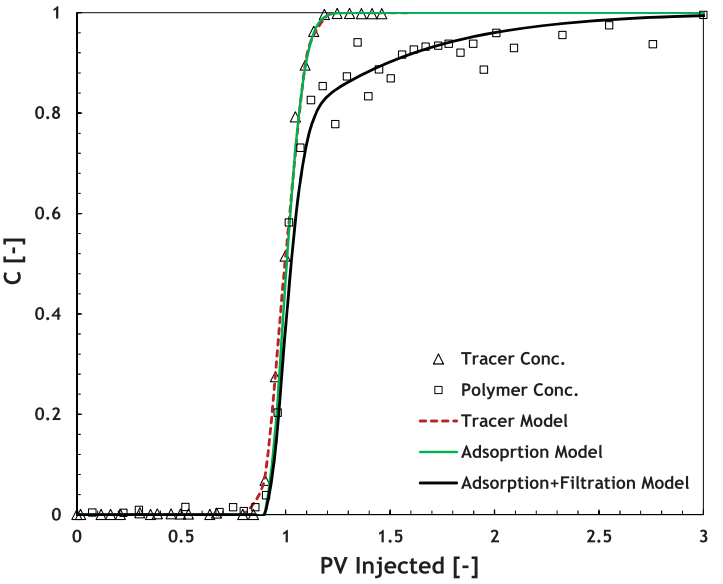

Figure 13. Comparison of the model with the experimental data (hydrolyzed polyacrylamide, HPAM, flow through a core with length of 30.5 cm, diameter of 3.81cm, $k = 2500$ mD, and $\varphi = 0.23$. The polymer was injected with velocity of 2 ft/d. The fit to the tracer data was obtained with a dispersivity length of 0.1 mm. The fit to the polymer data is obtained by setting $\lambda_0 = 0.55$ ft^{-1} and $\sigma_{max} = 0.016$ m^3/(m^3 PV). Data from *Lee* [2015].

4. Numerical Model for Polymer Flow With a Varying Filtration Coefficient

It is established that for a constant filtration coefficient, the polymer concentration in the effluent is recovered at a certain fraction of the injected concentration, depending on the value of λ. This occurs because of the steady state nature of the concentration solution, given by equation (17). Moreover, in this case, the pressure at the inlet continuously increases with no steady state behavior. In this section, the model consisting of equations (14a) and (14b) with a varying filtration coefficient in equation (6) is discussed.

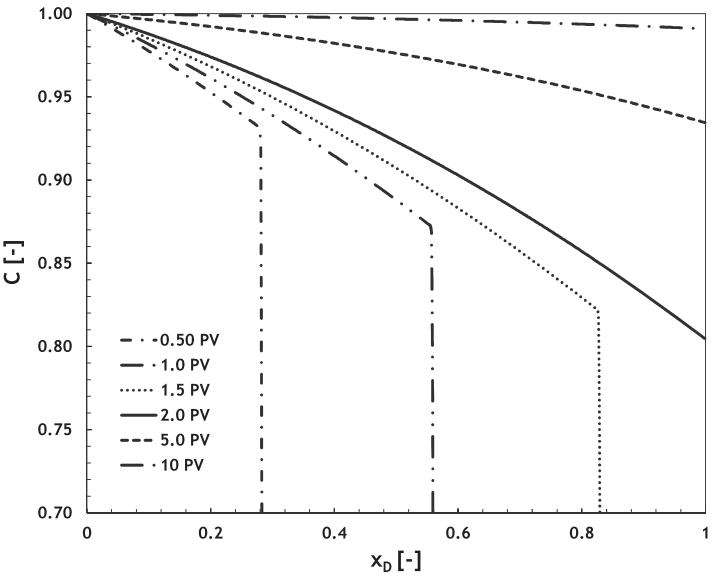

Figure 14. Flowing polymer concentration for the case with a nonconstant filtration coefficient expressed in equation (6) as a function of time (or pore volumes injected).

Figures 11 and 12 compare the experimental data with the proposed model with a varying filtration coefficient. In these experiments, polymer solutions were injected into cores initially saturated with brine. The match with the experimental data requires inclusion of dispersion in the model indicating local heterogeneities and/or fluid mixing in the cores. A dispersivity length was set to be about 1–5% of the total length of the core, which is in agreement with the available data and model [*Mahadevan et al*., 2003]. To obtain the dispersivity length, inclusion of tracers in the experiments is necessary. The tracer concentration can be used to extract the dispersion coefficient using the model. Then, the obtained dispersivity length can be fixed in the model to simulate the polymer concentration history at the outlet of the core. An example is shown in Figure 13. As mentioned earlier, the arrival of the front is mainly matched with the adsorption parameters while the slow recovery of the polymer production at the outlet is matched with the filtration theory indicating polymer entrapment. The values of the filtration coefficients obtained from the experimental data for polymer flow through porous media are smaller than those obtained for transport of particles. For such phenomena, the value of filtration coefficient ranges between 1 and 1000 m^{-1} [*Al-Abduwani et al*., 2005; *Kalantariasl*, 2014]. This is in agreement with the fact that the filtration rate depends on the size of the particles (or more accurately the ratio between the size of the pores and particles) and their distribution or concentration in the suspension. The size of the polymer molecules is typically less than size of the particles and therefore polymer molecules exhibit relatively smaller entrapment inside the porous medium.

Figure 14 shows the profile of the flowing polymer concentration for the case of filtration with a nonconstant filtration coefficient. The solution of this case consists of a continuous solution followed by a shock. The main difference of this solution with the solution in Figure 4 is the continuous change of the polymer concentration behind the front. This is shown in Figure 15. For the case of constant filtration coefficient, after polymer breakthrough, the concentration does not change and remains the

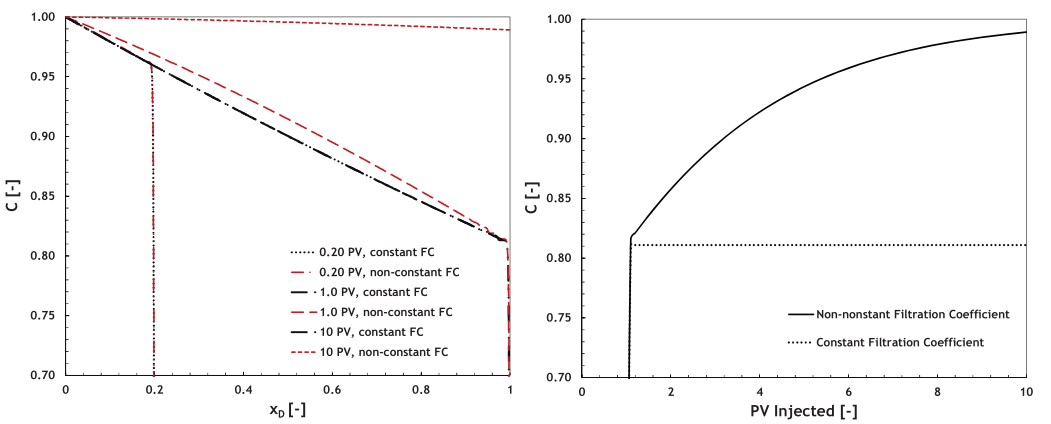

Figure 15. Comparison between the results of (right) constant and (left) varying filtration coefficient cases ($\lambda_0 = 0.5$ ft^{-1} for both cases and $\sigma_{max} = 0.018$ mol/m^3).

same, as a result of which the concentration remains constant at the outlet. However, when the filtration coefficient is not constant, the flowing concentration increases with time inside the porous medium, i.e., the concentration profile and history are both time dependent. Indeed because of the choice of the blocking function, the concentration of the flowing polymer increases, indicating that the amount of the entrapped polymer decreases. After a certain time, all the injected polymer will be in the flowing phase and the concentration at the outlet will be equal to the injected one.

The rate of the concentration recovery at the outlet depends on the value of λ_0 and σ_{max} in equation (6). With the increase of λ_0 more polymer molecules are retained in the porous medium and the polymer concentration at the breakthrough time decreases. After the breakthrough time, the polymer concentration rises and reaches a plateau value with the injection of certain pore volumes of the polymer solution. The pressure also stabilizes when concentration at the outlet reaches its plateau value, see figures in Appendix C. This is a major consequence of employing a nonconstant filtration coefficient; because as explained earlier, the assumption of constant filtration coefficient leads to a continuous pressure increase with a constant slope.

The kinetics of polymer entrapment could be very slow. Therefore, the pressure rise in the coreflood experiments can be very small and/or within the accuracy range of the pressure gauges, especially when short core plugs are used. For example, in Figure C2, detection of the pressure increase in the case with lower λ_0 can be difficult. Moreover, the experimental results cannot be easily up-scaled to field applications of polymer flooding. For reliable results and observable pressures, many pore volumes of polymer must be injected.

5. Conclusions

Polymer propagation in porous media is largely controlled by physical adsorption of the polymer molecules and the entrapment of the polymer macromolecules or suspended particles present in the makeup solvent. The polymer entrapment in the narrow pore throats can have a significant effect on its injection rate, if the polymer is not appropriately selected for a certain porous medium. The rate of the polymer retention depends on the flow rate, polymer concentration, and the polymer molecule and pore-throat sizes. In this paper, the combined effects of polymer adsorption and entrapment were studied. An equilibrium adsorption model was coupled to the filtration theory describing the kinetics of the polymer entrapment. The ensuing equation was then combined with the modified Darcy's law to calculate the pressure rise observed in some experiments. Analytical solutions were derived for the case of constant filtration coefficient, whereas the case of nonconstant filtration coefficient was solved numerically. The analytical and numerical modeling along with matching the examined experimental data allows the following conclusions to be made:

1. 1-D polymer flow with adsorption and constant filtration coefficient was solved analytically for dissolved, adsorbed, and entrapped concentrations and pressure drop across the porous medium.
2. Experimental data were successfully matched with the numerical model with a varying filtration coefficient suggesting that deep-bed filtration of the polymer molecules occurs simultaneously with polymer adsorption in the experiments examined in this paper.
3. Physical adsorption only affects the polymer front velocity and has no impact on the flowing polymer concentration, i.e., after the front breakthrough, the breakthrough polymer concentration is equal to the injected concentration.
4. For a constant filtration coefficient, the pressure continuously increases with a constant slope. The flowing polymer concentration behind a front remains constant and does not vary with time. The polymer concentration at the outlet does not reach its injected value and only a fraction of the injected polymer is produced at the plateau.
5. In the absence of physical adsorption, deep-bed filtration and capture of the polymer molecules do not affect the polymer front propagation. Nevertheless, when both filtration and adsorption are considered, filtration of the polymer molecules slows down the advancement of the front.
6. For the case of a nonconstant filtration coefficient, both pressure and concentration reach to a steady state solution after a certain time. The equilibration time depends on the values of λ_0 and σ_{max} in equation (6).

7. Polymer retention is a time-dependent process. This indicates that a reliable assessment of the polymer injectivity in porous media may need injecting many pore volumes of the polymer solution.

Appendix A: Solution for the Case With a Linear Dependence Between the Retained and Flowing Concentrations

In this section, the solution of the equations considering Henry's law for adsorption is presented. In this case, equation (8) becomes

$$\hat{C}=\Gamma C, \tag{A1}$$

where, Γ is the slope of the linear dependency between the concentration of polymer on the rock surface and in the aqueous solution. The initial and boundary conditions are the same as described by equations (9) and (10). Equations (5) and (6) can be solved together with equation (A1) to obtain the flowing and the entrapped polymer concentrations. Solution of the flowing polymer concentration will be the same, i.e., equal to equation (14).

The expression for the front trajectory in this case becomes

$$t_f=(1+\Gamma)x_D. \tag{A2}$$

Therefore, the polymer breakthrough at the core outlet occurs at:

$$t_{BT}=1+\Gamma. \tag{A3}$$

The concentration profile is given by equations (14b) and (A2):

$$C(x_D,t_D)=\begin{cases} e^{-\Lambda x_D}, & t_D>1+\Gamma \\ 0, & t_D<1+\Gamma \end{cases}. \tag{A4}$$

Substitution of equation (A2) into equation (23) leads to

$$S(x_D,t_D)=\Lambda(t_D-x_D(1+\Gamma\ ))e^{-\Lambda x_D}. \tag{A5}$$

A1. Calculation of the Pressure Drop

The second integral in the right-hand side of equation (25) is equal to

$$\int_0^{x_{Df}}(1+MC)\hat{C}dx_D=-\frac{\Gamma}{\Lambda}\left(e^{-\Lambda x_{Df}}-1+\frac{M}{2}\left(e^{-2\Lambda x_{Df}}-1\right)\right). \tag{A6}$$

The third integral in the right-hand side of equation (25) before the polymer breakthrough is

$$\int_0^{x_{Df}}(1+MC)Sdx_D=t_D\left(1-e^{-\Lambda x_{Df}}+\frac{M}{2}\left(1-e^{-2\Lambda x_{Df}}\right)\right)+\frac{1+\Gamma}{\Lambda}e^{-\Lambda x_{Df}}\left(1+\Lambda x_{Df}+\frac{M}{4}e^{-\Lambda x_{Df}}(2\Lambda x_{Df}+1)\right)-\frac{1+\Gamma}{\Lambda}\left(1+\frac{M}{4}\right). \tag{A7}$$

Therefore, the pressure drop before the breakthrough can be calculated from

$$\begin{aligned}\Delta P=x_{Df}+\frac{M}{\Lambda}\left(1-e^{-\Lambda x_{Df}}\right)\ &+\left(\frac{R\phi c_0\Gamma}{\Lambda}+\beta\phi c_0 t_D\right)\left(1-e^{-\Lambda x_{Df}}+\frac{M}{2}\left(1-e^{-2\Lambda x_{Df}}\right)\right)\\ &+\beta\phi c_0\frac{1+\Gamma}{\Lambda}\left[e^{-\Lambda x_{Df}}\left(1+\Lambda x_{Df}+\frac{M}{4}e^{-\Lambda x_{Df}}(2\Lambda x_{Df}+1)\right)-\left(1+\frac{M}{4}\right)\right].\end{aligned} \tag{A8}$$

After the polymer breakthrough, the integration in x_D is performed from zero to one, and the pressure can be calculated by inserting $x_{Df}=1$ in equation (29), i.e.,

$$\Delta P=1+\frac{M}{\Lambda}\left(1-e^{-\Lambda}\right)+\left(\frac{R\phi c_0\Gamma}{\Lambda}+\beta\phi c_0 t_D\right)\left(1-e^{-\Lambda}+\frac{M}{2}\left(1-e^{-2\Lambda}\right)\right)+\beta\phi c_0\frac{1+\Gamma}{\Lambda}\left[e^{-\Lambda}\left(1+\Lambda+\frac{M}{4}e^{-\Lambda}(2\Lambda+1)\right)-\left(1+\frac{M}{4}\right)\right]. \tag{A9}$$

Appendix B: Details of the Numerical Solution

The continuity of mass for the polymer component in association with Darcy's law is expressed in terms of the overall volume of the polymer per unit pore volume ($\hat{c}_p$) as (p subscript stands for polymer)

$$\frac{\partial}{\partial t}\left(\rho_p\left[\phi\sum_{l=1}^{n_p}S_l c_{pl}+\hat{c}_p+\sigma\right]\right)+\vec{\nabla}.\left[\sum_{l=1}^{n_p}\rho_p\left(c_{pl}\vec{u}_l-\vec{\bar{D}}_{pl}\right)\right]=Q_p \quad l=1 \text{ and } 2. \tag{B1}$$

where c_{pl}, $\hat{c}_p$, and σ are polymer concentration in phases l, adsorbed polymer concentration on the rock, and the retained polymer concentration due to filtration. ρ_p is polymer density, n_p is number of phases ($l=1$ is aqueous phase, and $l=2$ is oleic phase), S_l is saturation of phase l, and Q_p is injection/production rate of the polymer component. In this study, we deal with single-phase flow. $\vec{\bar{D}}_p$is the dispersive flux and is assumed to have a Fickian form:

$$\vec{\bar{D}}_{pl}=\phi S_l\vec{\bar{K}}_{kl}.\vec{\nabla}C_{kl}. \tag{B2}$$

The dispersion tensor $\vec{\bar{K}}_{kl}$ including the molecular diffusion (D_{kl}) is calculated as follows

$$\vec{\bar{K}}_{klij}=\frac{D_{kl}}{\tau}\delta_{ij}+\frac{\alpha_{Tl}}{\phi S_l}|\vec{u}_l|\delta_{ij}+\frac{(\alpha_{Ll}-\alpha_{Tl})}{\phi S_l}\frac{u_{li}u_{lj}}{|\vec{u}_l|}, \tag{B3}$$

where α_{Ll} and α_{Tl} are phase l longitudinal and transverse dispersivities, τ is the tortuosity, u_{li} and u_{lj} are the components of Darcy flux of phase l in direction i and j, and δ_{ij} is the Kronecker function. $|\vec{u}_l|$ is the magnitude of vector flux for each phase and is computed as

$$|\vec{u}_l|=\sqrt{(u_{xl})^2+(u_{yl})^2+(u_{zl})^2}. \tag{B4}$$

The phase flux from Darcy's law is

$$\vec{u}_l=-\frac{k_{rl}\vec{\bar{k}}}{\mu_l}\left(\vec{\nabla}P_l-\gamma_l\vec{\nabla}h\right)$$

where $\vec{\bar{k}}$ is intrinsic permeability tensor and h is vertical depth. k_{rl} is relative permeability phase of l, μ_l is viscosity for phase l, and γ_l is specific weight for phase l.

The rate of polymer filtration is defined as

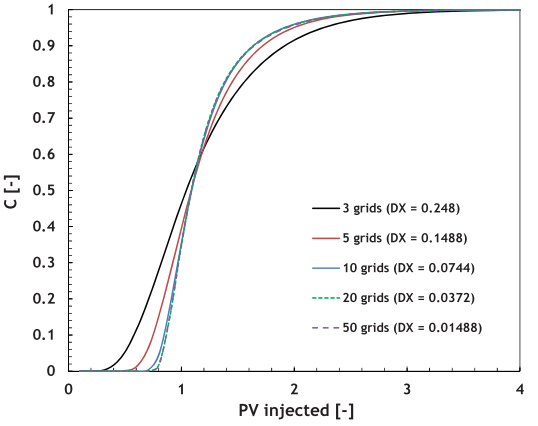

Figure B1. Effect of gridblock size on the solution of the concentration history.

$$\frac{d\sigma}{dt} = \lambda \phi S_l u_l c_{pl}$$

where λ is the filtration coefficient. λ can be either constant or variable during the filtration process. For the variable λ, filtration rate depends on the retained concentration of the polymer

$$\lambda(\sigma) = \lambda_0 \left(1 - \frac{\sigma}{\sigma_{\max}}\right)$$

where λ_0 is the filtration coefficient at zero polymer retention, and $\sigma_{\max}$ is maximum polymer retention.

In presence of polymer, the viscosity of the aqueous phase is calculated from Carreau's model [*Carreau*, 1968].

The above system of equations along with the pressure equation was discretized using finite difference approach and was solved in IMPEC (implicit pressure explicit concentration) scheme.

To avoid the numerical dispersion, we use small gridblock size to minimize the effect of numerical dispersion. We did sensitivity analysis to gridblock size until we did not see any changes in polymer concentration (Figure B1).

Appendix C: Effects of λ_0 and σ_{max} in Equation (6) on the Concentration and Pressure Histories

Figures C1 and C2 show the effect of λ_0 on the history of the flowing polymer concentration and the pressure, respectively. The increase in the value of λ_0 has three important effects: (1) it delays the breakthrough of the polymer when combined with adsorption, (2) it significantly increases the rate of the polymer recovery from the breakthrough value to unity, and (3) it increases the rate of pressure rise.

Figures C3 and C4 show the effect of σ_{max} on the history of the flowing polymer concentration and pressure, respectively. σ_{max} has no significant effect on the polymer breakthrough; however, at any given time, the polymer concentration at the outlet increases with decreasing σ_{max}. For smaller values of σ_{max}, the entrapment sites are occupied faster, and consequently, the concentration and pressure are stabilized in a shorter time.

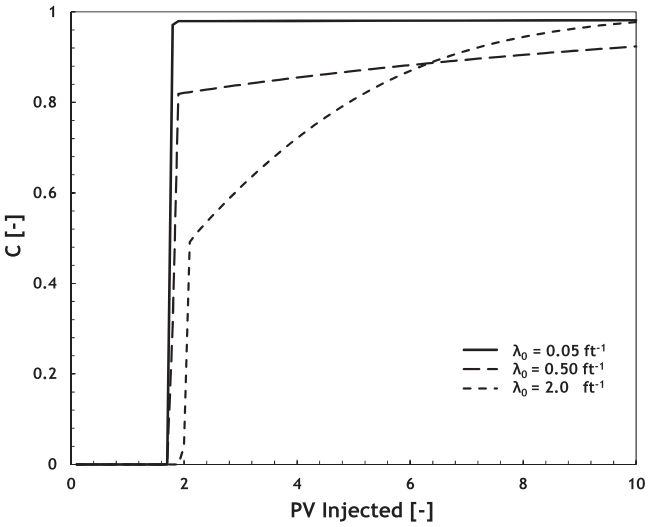

Figure C1. Effect of maximum filtration coefficient (the filtration coefficient at zero polymer retention, λ_0, in equation (6)) on the history of the effluent concentration. The maximum retained polymer concentration, σ_{max}, is kept equal to 0.05 mol/m^3.

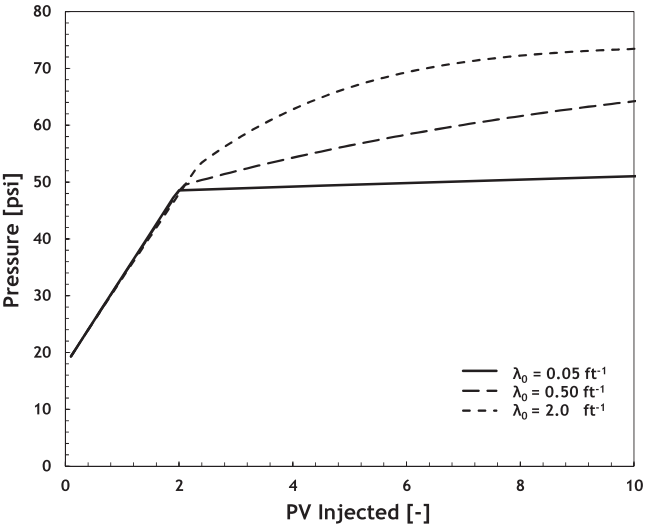

Figure C2. Effect of maximum or reference filtration coefficient at zero polymer retention (λ_0 in equation (6)) on the pressure history. The maximum retained polymer concentration, $\sigma_{max,}$ is kept equal to 0.05 mol/m^3.

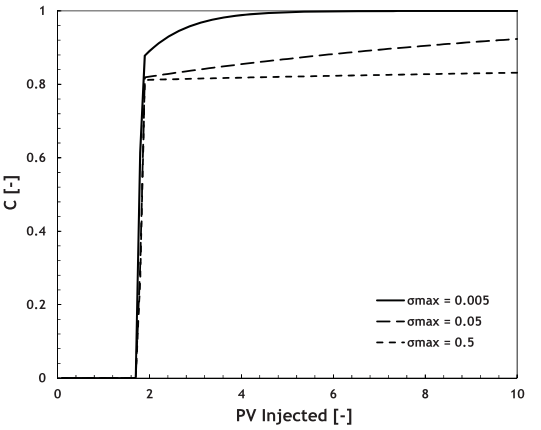

Figure C3. Effect of σ_{max} (the maximum retained polymer concentration as described in equation (6)) on the history of the effluent concentration (C). The reference filtration coefficient at zero polymer retention (λ_0) is kept equal to 0.50 m^{-1}.

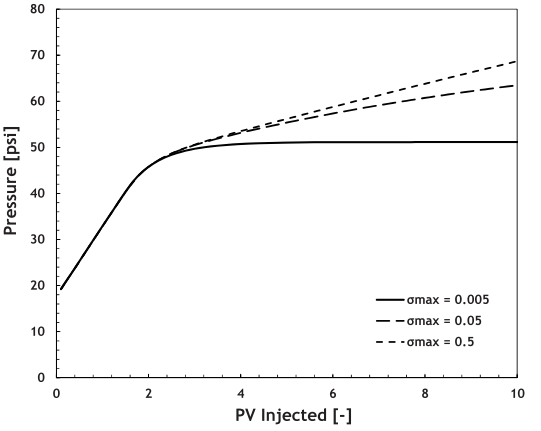

Figure C4. Effect of σ_{max} (the maximum retained polymer concentration as described in equation (6)) on the pressure history. The reference filtration coefficient at zero polymer retention (λ_0) is kept equal to 0.50 m^{-1}.

Notation

b	Langmuir polymer adsorption parameter.
c	polymer concentration in aqueous phase, L^3 polymer/L^3 aqueous phase or mass polymer/mass aqueous phase.
C	dimensionless polymer concentration in aqueous phase.
$\hat{c}$	adsorbed polymer concentration, L^3 polymer/L^3 pore volume.
$\hat{C}$	dimensionless adsorbed polymer concentration.
$\hat{C}_{max}$	maximum dimensionless adsorbed-polymer concentration.
c_o	injection concentration, L^3 polymer/L^3 aqueous phase.
k	permeability, L^2
L	core length, L
p	pressure, $M\,L^{-1}\,T^{-2}$.
P	dimensionless pressure.
R	permeability-reduction (or resistance) factor due to polymer adsorption.
S	dimensionless trapped (retained) polymer concentration.
t	time, T
t_{BT}	breakthrough time.
t_D	dimensionless time.
t_{Df}	dimensionless front trajectory.
t_f	front trajectory, T.
u	aqueous phase Darcy velocity, $L\,T^{-1}$.
Λ	dimensionless filtration coefficient.
x_D	dimensionless distance.
x_{Df}	dimensionless front position.
x_f	front position, L.
β	formation-damage coefficient.
λ	filtration coefficient, L^{-1}.
λ_o	filtration coefficient at zero polymer retention, L^{-1}.
σ	trapped (retained) polymer concentration, L^3 polymer/L^3 bulk volume.
σ_{max}	maximum trapped (retained) polymer concentration, L^3 polymer/L^3 bulk volume.
ϕ	porosity.
μ	viscosity, $M\,L^{-1}\,T^{-1}$.
μ_p	polymer viscosity, $M\,L^{-1}\,T^{-1}$.
μ_w	water viscosity, $M\,L^{-1}\,T^{-1}$.

Acknowledgments
The authors thank Gerard Glasbergen (Shell) for his valuable comments on the draft of this paper. We thank Shell Global Solutions International for granting permission to publish this work. The data presented in this paper can be requested from the corresponding author (r.farajzadeh@tudelft.nl).

References

Al-Abduwani, F. A. H., R. Farajzadeh, W. van den Broek, P. K. Currie, and P. L. J. Zitha (2005), Filtration of micron-sized particles in granular media revealed by x-ray computed tomography, *Rev. Sci. Instrum.*, *76*(10), 103704.

Barenblatt, G. I., V. M. Entov, and V. M. Ryzhik (1989), *Theory of Fluid Flows Through Natural Rocks*, Kluwer Acad., London, U. K.

Bedrikovetsky, P. (1993), *Mathematical Theory of Oil & Gas Recovery, With Applications to Ex-USSR Oil & Gas Condensate Fields*, Kluwer Acad., London.

Bedrikovetsky, P. (2008), Upscaling of stochastic micro model for suspension transport in porous media, *Transp. Porous Media*, *75*(3) 335–369.

Bengtsson, G., and L. Ekere (2001), Predicting sorption of groundwater bacteria from size distribution, surface area, and magnetic susceptibility of soil particles, *Water Resour. Res.*, *37*(6), 1795–1812.

Bold, S., S. Kraft, P. Grathwohl, and R. Liedl (2003), Sorption/desorption kinetics of contaminants on mobile particles: Modeling and experimental evidence, *Water Resour. Res.*, *39*(12), 1329, doi:10.1029/2002WR001798.

Carreau, P. J. (1968), Rheological equations from molecular network theories, PhD dissertation, Univ. of Wis., Maddison.

Clemens, T., M. Deckers, M. Kornberger, T. Gumpenberger, and M. Zechner (2013), Polymer solution injection - near wellbore dynamics and displacement efficiency, pilot test results, Matzen Field, Austria, *Soc. Petrol. Eng.*, doi:10.2118/164904-MS.

Cohen, Y., and F. R. Christ (1986), Polymer retention and adsorption in the flow of polymer solutions through porous media, *SPE Reservoir Eng.*, *1*, 113–118.

Dake, L. P. (1978), *Fundamentals of Reservoir Engineering*, Elsevier, N. Y.

Dann, M. W., D. B. Burnett, and L. M. Hall (1982), Polymer performance in low permeability reservoirs, paper SPE 10615 presented at the SPE Sixth International Symposium on Oilfield and Geothermal Chemistry, Soc. of Pet. Eng., Dallas, Tex., 25–27 Jan.

Denys, K. F. J. (2003), Flow of polymer solution through porous media, PhD dissertation, Delft Univ. of Technol., Delft, Netherland.

Dominguez, J. G., and G. P. Willhite (1977), Retention and flow characteristics of polymer solutions in porous media, *Soc. Pet. Eng. J.*, *17*(2), 111–121.

Dykstra, H., and R. L. Parsons (1950), The prediction of oil recovery by waterflood, Secondary recovery of oil in the United States, in Principles and Practice, 2d ed., pp. 160–174, Am. Pet. Inst., N. Y.
Glasbergen, G., D. Wever, E. Keijzer, and R. Farajzadeh (2015), Injectivity loss in polymer floods: Causes, preventions and mitigations, paper SPE 175383 presented at the SPE Kuwait Oil & Gas Show and Conference, Soc. of Pet. Eng., Mishref, Kuwait, 11–14 Oct.
Gogarty, W. B. (1967), Mobility control with polymer solutions, *Soc. Pet. Eng. J.*, *7*(2), 161–173.
Green, D. W., and G. P. Willhite (1998), *Enhanced Oil Recovery, SPE Textbook Ser.*, vol. 6, Soc. of Pet. Eng., Richardson, Tex.
Hirasaki, G. J., and G. A. Pope (1974), Analysis of factors influencing mobility and adsorption in the flow of polymer solutions through porous media, *Soc. Pet. Eng. J.*, *14*, 337–346.
Huh, C., E. A. Lange, and W. J. Cannella (1990), Polymer retention in porous media, paper SPE 20235 presented at the SPE/DOE Seventh Symposium on Enhanced Oil Recovery, Soc. of Pet. Eng., Tulsa, Okla., 22–25 April.
Kalantariasl, A., A. Zeinijahromi, and P. Bedrikovetsky (2014), Axi-symmetric two-phase suspension-colloidal flow in porous media during water injection, *Ind. Eng. Chem. Res.*, *53*(40), 15763–15775.
Lake, L. W., S. L. Bryant, and A. N. Araque-Martinez (2003), *Geochemistry and Fluid Flow, Developments in Geochemistry*, Elsevier Sci, Amsterdam, Netherlands.
Lake, L. W., R. T. Johns, W. R. Rossen, and G. A. Pope (2014), *Fundamentals of Enhanced Oil Recovery*, Soc. of Pet. Eng., Richardson, Tex.
Landau, L. D., and E. M. Lifshitz (1987), Fluid mechanics, *Course of Theoretical Physics*, Pergamon Press.
Lee, J. J., and G. G. Fuller (1985), Adsorption and desorption of flexible polymer chains in flowing systems, *J. Colloid Interface Sci.*, *103*(2), 569–577.
Lee, V. B. (2015), The development and evaluation of polymers for enhanced oil recovery, MSc thesis, Univ. of Texas at Austin, Austin.
Lotfollahi, M., R. Farajzadeh, M. Delshad, Kh. Al-Abri, B. W. Wassing, K. Awan, R. Mjeni, and P. Bedrikovetsky (2016), Mechanistic simulation of polymer injectivity during field tests, *SPE J.*, in press.
Maerker, J. M. (1973), Dependence of polymer retention on flow rate, *J. Pet. Technol.*, *25*(11), 1307–1308.
Mahadevan, J., L. W. Lake, and R. T. Johns (2003), Estimation of true dispersivity in field-scale permeable media, *SPE J.*, *8*(3), 272–279.
Manichand, R. N., and R. S. Seright (2014), Field vs. laboratory polymer retention values for a polymer flood in Tambaredjo field, *SPE Reservoir Eval. Eng.*, *17*, 1–12.
Masuda, Y., K. Tang, M. Miyazawa, and S. Tanaka (1992), 1 D simulation of polymer flooding including the viscoelastic effect of polymer solution, *SPE Reservoir Eng.*, *7*(2), 247–252.
McDowell-Boyer, L. M., J. R. Hunt, and N. Sitar (1986), Particle transport through porous media, *Water Resour. Res.*, *22*(13), 1901–1921.
Seright, R. S., J. Mac Seheult, and T. Talashek (2009), Injectivity characteristics of EOR polymers, *SPE Reservoir Eval. Eng.*, *12*(5), 783–792.
Sheng, J. J., B. Leonhardt, and N. Azri (2015), Status of polymer-flooding technology, *Soc. Petrol. Eng.*, doi:10.2118/174541-PA.
Sim, Y., and C. V. Chrysikopoulos (1995), Analytical models for one-dimensional virus transport in saturated porous media, *Water Resour. Res.*, *31*(5), 1429–1437.
Soltanov, H. (2013), A note on the Goursat problem for a multidimensional hyperbolic equation, *Contemporary Anal. Appl. Math.*, *1*(2), 98–106.
Sorbie, K. S. (1991), *Polymer-Improved Oil Recovery*, CRC Press, Boca Raton, Fla.
Szabo, M. T. (1975a), Laboratory investigations of factors influencing polymer flood performance, *Soc. Pet. Eng. J.*, *15*, 338–346.
Szabo, M. T. (1975b), Some aspects of polymer retention in porous media using a C14-tagged hydrolyzed polyacrylamide, *Soc. Pet. Eng. J.*, *15*(4), 323–337.
Szabo, M. T. (1979), An evaluation of water-soluble polymers for secondary oil recovery—Parts 1 and 2, JPT *J. Pet. Technol.*, *31*(5), 561-570.
Vaz, A. S., Jr., P. Bedrikovetsky, C. J. A. Furtado, and A. L. S. de Souza (2010), Well injectivity decline for nonlinear filtration of injected suspension: Semi-analytical model, *J. Energy Resour. Technol.*, *132*, 1–9.
Velza, S., D. W. Peaceman, and E. I. Sandvik (1974), Evaluation of polymer flooding in a layered reservoir with crossflow, retention, and degradation, *Soc. Pet. Eng. J.*, *16*, 82–96.
Yerramilli, S. S., R. C. Yerramilli, and P. L. J. Zith (2013), Novel insight into polymer injectivity for polymer flooding, paper SPE-165195-MS presented at SPE European Formation Damage Conference & Exhibition, Soc. of Pet. Eng., Noordwijk, Netherlands, 5–7 June.
Zaitoun, A., N. Kohler, D. Bossie-Codreanu, and D. Denys (1999), Water shutoff by relative permeability modifiers: Lessons from several field applications, paper SPE-56740-MS presented at SPE Annual Technical Conference and Exhibition, Soc. of Pet. Eng., Houston, Tex., 3–6 Oct.
Zhang, G., and R. Seright (2014), Effect of concentration on HPAM retention in porous media, *SPE J.*, *19*, 373–380.
Zitha, P. L. J., and C. W. Botermans (1998), Bridging-adsorption of flexible polymers in low permeability porous media, *SPE Prod. Facil.*, *13*(1), 15–20.
Zitha, P. L. J., K. G. S. van Os, and K. F. J. Denys (1998), Adsorption of linear flexible polymer during laminar flow through porous media: Effect of concentration, paper SPE-39675-MS presented at the SPE/DOE Improved Oil Recovery Symposium, Soc. of Pet. Eng., Tulsa, Okla., 19–22 April.